

srika2

by Mohammad Alauhdin 132307273

Submission date: 10-Jun-2024 08:16PM (UTC+0700)

Submission ID: 2333824504

File name: srika2.pdf (639.2K)

Word count: 8315

Character count: 43352

The Catalytic Activity of TCA-Modified Indonesian Natural Zeolite During the Esterification of Sengon Wood Bio-Oil

Sri Kadarwati^{1,*}, Riska Nurfirda Annisa², Evalisa Apriliani³,
Cepi Kurniawan⁴ and Samuel Budi Wardhana Kusuma⁵

Department of Chemistry, Faculty of Mathematics and Natural Sciences, Universitas Negeri Semarang, Semarang 50229, Indonesia

(*Corresponding author's e-mail: srika@mail.unnes.ac.id)

Received: 8 April 2022, Revised: 3 June 2022, Accepted: 10 June 2022, Published: 2 December 2022

Abstract

The bio-oil produced from the pyrolysis of biomass is highly corrosive due to the high content of organic acids. These organic acids could be removed through an appropriate upgrading process, i.e., esterification using alcohols to form less polar esters. In this study, the bio-oil used as the feedstock in the esterification was produced from the pyrolysis of Sengon wood with a particle size of 297 μm at 600 °C. The esterification was performed at 70 °C in the presence of a trichloro acetic acid (TCA)-modified Indonesian H-zeolite catalyst with various weight ratios of bio-oil-to-methanol at reaction times under a constant stirring rate of 500 rpm. The esterification progress was indicated by the decrease in the total acid number of the bio-oil after esterification. No significant coke formation (< 0.05 wt%) was observed indicating that the suppression of repolymerisation could be achieved. This study showed that the esterification underwent in a fast rate, indicated by the decrease in the total acid number of the bio-oil by 47.85 % only over a 15-min esterification. Compared to the uncatalysed esterification, the TCA/zeolite-catalysed esterification showed a higher decrease in the total acid number of the bio-oil up to 65.83 %, due to the conversion of the carboxylic acids to esters.

Keywords: Esterification, Sengon wood bio-oil, TCA-modified Indonesian zeolite, Total acid number

Introduction

The fossil fuel depletion has promoted the exploration of new renewable energy resources. Biomass has been considered as a promising renewable energy resource due to its high availability, its environmentally friendly properties and its zero competition with food sector [1]. A liquid fuel could be produced as the main product from the fast pyrolysis of biomass [2] that is well known as bio-oil or pyrolysis oil. Sengon wood, as an abundantly available feedstock in Indonesia was used in this study for bio-oil production. Sengon wood contains lignin, cellulose, and hemicellulose of 26.1, 45.4 and 21.0 % and respectively [3]. The high content of cellulose in Sengon wood would result in the high yield of bio-oil [4], allowing a sustainable starting material for liquid fuel production.

The bio-oil produced from the pyrolysis of biomass could be used as a fuel for boilers, stationary as well as sterling engines [5]. However, the bio-oil cannot be directly used as a fuel for transportation due to several unfavourable properties such as high water content leading to low calorific value and high oxygen content resulting in highly instable properties [6]. In addition, the bio-oil contains high amount of organic acids making it highly corrosive and causing a big challenge during its use as a fuel or its compatibility during further processing in the biorefinery [7]. A bio-oil upgrading is required for the bio-oil to meet the requirements as liquid transportation fuels [8].

Esterification has been reported to show a great potential as bio-oil upgrading technique to reduce the acids content of the bio-oil [9]. It converts the organic acids in the bio-oil to e.g., esters in the presence of alcohols and acid catalysts [10]. The use of solid acid catalysts during the esterification of bio-oil has been considered more beneficial in comparison with that of homogeneous catalysts due to the easy separation resulting in a more efficient and cost-effective process [11]. Several solid acid catalysts such as ion exchange resins [12], modified zirconia [13,14], Amberlysts [15-17], acid modified rice husk ash [18], and heteropoly acids [19] have been used as a catalyst in the esterification of the "real" bio-oil as well as model compounds mimicking bio-oil. In addition, zeolite-based catalysts have been reported to show a great potential as a catalyst for esterification of bio-oil [20-24].

A special attention has been paid to Indonesian natural zeolite primarily in related to its application as a catalyst for bio-oil upgrading. It has a good porosity and modifiable Brønsted acid sites [25] at its surface to anticipate the complicated compositions and behaviour of the bio-oil during the esterification. The modification [10] of Brønsted acid sites at the Indonesian zeolite surface to improve the Brønsted acidity could enhance the catalytic activity of Indonesian zeolite during the esterification of the bio-oil.

The Brønsted acidity of the Indonesian zeolite could be improved by strong acid modification, e.g., trichloroacetic acid (TCA) resulting in the zeolite with a better Brønsted acidity [26]. However, the application of TCA-modified Indonesian natural zeolite as a catalyst for esterification of bio-oil produced from the fast pyrolysis of Sengon wood was rare. More studies to investigate the activity of the TCA-modified Indonesian natural zeolite are necessary to evaluate its potential as a catalyst for the bio-oil esterification. This study focused on the esterification [17] of the bio-oil produced from the fast pyrolysis of Sengon wood sawdust with various weight ratios of bio-oil-to-methanol and reaction times to investigate the esterification behaviour of organic acids in the bio-oil primarily acetic acid in the presence of methanol and TCA-modified Indonesian natural zeolite as a solid acid catalyst.

Materials and methods

Preparation and characterisation of a TCA-modified Indonesian natural zeolite catalyst

The Indonesian natural zeolite from Wonosari, Yogyakarta, Indonesia was used as a starting material of the zeolite catalyst. It was purchased from CV. SSGT Zeolite, Indonesia. The natural zeolite was prepared as previously reported [24]. Briefly, the natural zeolite with a particle size range of 100 - 120 µm was activated using sequent chemical and physical activation method. Prior to activation process, the natural zeolite was washed in distilled water and dried at 110 °C for 3 h to allow the physical contaminant removal. "Pre-treated zeolite" corresponds the natural zeolite from this pre-treatment step.

The natural zeolite was chemically treated using 1 % HF, 6 N HCl and 1 N NH₄Cl solutions (prepared from 50 % HF, 37 % HCl, and solid NH₄Cl, obtained from E. Merck, respectively) in a sequence. This chemical activation was followed with a physical activation, i.e., calcination of the natural zeolite sample at 500 °C under nitrogen atmosphere to produce "H-zeolite" catalyst [24].

The modification of the "H-zeolite" catalyst with chloroacetic acid was carried out as reported by Ávila *et al.* [6] with some adjustment. A 5 g of TCA was dissolved in 9 mL of demineralised water in an Erlenmeyer flask. A 10 g of "H-zeolite" was added in the TCA solution. The mixture [6] is then heated at 80 °C under a continuous stirring with a low stirring rate of 100 rpm until no water left. The solid obtained was dried in an oven at 110 °C for 2 h resulting in the "TCA/H-zeolite" catalyst.

The formation of the "TCA/H-zeolite" catalyst was confirmed based on the appearance of characteristics vibration peaks at wavenumbers of 830 and 680 cm⁻¹ (the stretching vibration of C-Cl bonds) [26] in the IR spectrum. The IR spectrum of the "TCA/H-zeolite" catalyst was obtained using a Perkin-Elmer Frontier Spotlight 200 type-Fourier transform infrared spectrophotometer. In addition, the possible change in the crystalline structure of Indonesian natural zeolite was evaluated using a PANalytical Xpert 3 Powder X-ray diffractometer.

The surface properties of the "TCA/H-zeolite" catalyst were characterised using a Quantachrome Nova 1,200e surface area analyser. The specific surface area, total pore volume and average pore radius were determined using a BET-BJH isotherm adsorption. Moreover, the acidity of the "TCA/H-zeolite" catalyst was determined using an ammonia adsorption. The amount of ammonia adsorbed at the catalyst surface was assigned as the total acidity of the catalyst in mmol ammonia per gram catalyst. This quantitative measurement of the catalyst acidity was combined with the analysis of the chemical functionalities of the catalyst to confirm the presence of the new bonds of ammonia with the Lewis and Brønsted acid sites at the catalyst surface at wavenumbers of 1,640, 1,550 and 1,450 cm⁻¹.

Catalytic esterification of sengon wood bio-oil

The esterification of the bio-oil with methanol in the presence of "TCA/H-zeolite" catalyst was carried out in a batch reactor system equipped [25] with a temperature monitor and magnetic stirrer. The esterification was conducted at 70 °C, with a catalyst loading of 10 wt%, a stirring rate of 100 rpm, and various weight ratios of bio-oil-to-methanol of 1:1, 2:1, 1:2 and 1:3. The Sengon wood bio-oil used in the esterification process was produced from the pyrolysis of Sengon wood sawdust with a particle size of 297 µm [17] at 600 °C using a fixed-bed pyrolyser as previously reported [24]. The esterification with a weight ratio of bio-oil-to-methanol which gave the highest decrease in the total acid number of the bio-oil after esterification underwent that with various esterification times of 15, 30, 45 and 60 min.

After each experiment, the mixture of liquid esterification products and possible remaining reactants was recovered and designated as the esterified bio-oil. The coke formation was determined based on the weight difference of solid catalyst before and after the esterification. The yield of coke was calculated using Eq. (1) to close the mass balance. W'_{cat} and W^0_{cat} are designated as the weight of the "TCA/H-zeolite" catalyst after and before the esterification of the bio-oil, respectively, while $W_{bio-oil\ fed}$ is the weight of the bio-oil fed in each esterification experiment.

$$Coke\ yield = \frac{W'_{cat} - W^0_{cat}}{W_{bio-oil\ fed}} \times 100\% \quad (1)$$

Characterisation of the bio-oil after esterification

The esterified bio-oil after each esterification experiment was characterised, including the density, viscosity and total acid number. The density and viscosity of the esterified bio-oil were determined using a gravimetric method by means of a pycnometer and an Ostwald viscometer, respectively.

The total acid number (TAN) of the esterified bio-oil was measured using an SNI 01-3555-1998 procedure as follows. The bio-oil sample was dissolved in acetone to 96 wt% clear solution of bio-oil. A 2.5 g of the bio-oil solution was heated to boil and added with 2-3 drops of phenolphthalein solution. The titration of the bio-oil solution was conducted using 0.1 N KOH solution until a light red colour appeared. The total acid number of the esterified bio-oil was calculated using Eq. (2). MW_{KOH} , N_{KOH} , and V_{KOH} are designated as the molecular weight, normal concentration and volume of KOH solution, respectively. Meanwhile, W_{sample} and *dilution* are designated as the weight of the sample and the magnitude of dilution employed during the measurement of TAN.

$$TAN = \frac{MW_{KOH} \times N_{KOH} \times V_{KOH}}{W_{sample}} \times dilution \quad (2)$$

Results and discussion

The characteristics of TCA/H-zeolite catalyst

The important properties of the TCA/H-zeolite catalyst prepared in this study was investigated, including the chemical functionalities, the possible change in the crystalline structure, the surface porosity, and the total acidity. The chemical functionalities of the TCA/H-zeolite catalyst were represented by the spectra in **Figure 1**. The general featured functionalities of the zeolite with aluminosilicate framework were shown by the appearance of a vibration peak -OH groups at 3,200 - 3,600 cm^{-1} . In addition, bending vibrations of Al-OH/Si-OH were observed at 1,650 - 1,400 cm^{-1} , while stretching vibrations of Si-O/Al-O were observed at wavenumbers of 1,250 - 950 and 820 - 650 cm^{-1} .

The success of the zeolite modification with TCA was confirmed by the appearance of stretching vibrations of C-Cl bonds at wavenumbers of 840 and 690 cm^{-1} [26] at the IR spectrum of the TCA/H-zeolite catalyst (**Figure 1(c)**). These vibrations indicated the chemical interaction between TCA and the -OH groups of the zeolite.

The change in the crystalline structure of the zeolite over subsequent chemical and physical treatment as well as TCA modification was evaluated through the XRD patterns of the pre-treated zeolite, H-zeolite and the TCA/H-zeolite catalysts, as shown in **Figure 2**. The similar XRD patterns and peak intensity in **Figure 2** indicated that the zeolite did not undergo a significant change in the crystalline structure over the subsequent treatments. Moreover, the intensity of the 3 highest peaks denoted that the mordenite mineral structure was predominant in the zeolite catalysts.

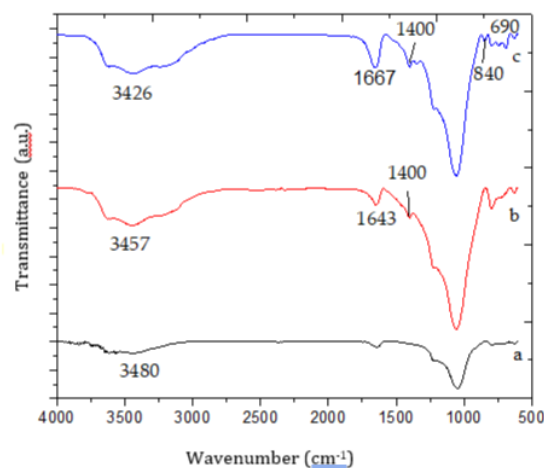


Figure 1 IR spectra of a) pre-treated zeolite, b) H-zeolite and c) TCA/H-zeolite.

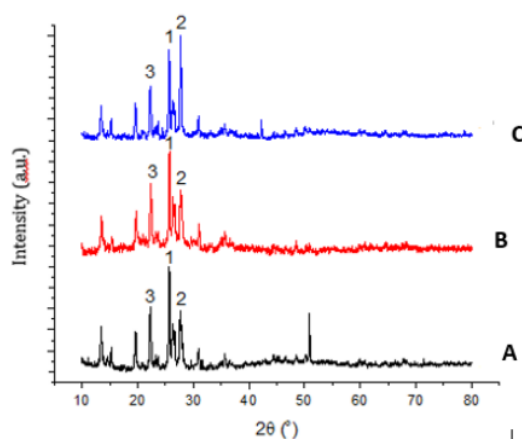


Figure 2 The diffraction patterns of a) pre-treated zeolite, b) H-zeolite and c) TCA/H-zeolite.

The measurement of the total (Lewis and Brønsted) acidity of the TCA/H-zeolite catalyst was performed to support the data of IR spectra indicating the success of the zeolite modification with TCA. The significant increase of the total acidity of the TCA/H-zeolite catalyst would further evidence of the success modification in this study. In addition, the enhanced total acidity of the TCA/H-zeolite catalyst would promote a better esterification process as this acid active sites would play important roles in catalysing the esterification of bio-oil with methanol [13].

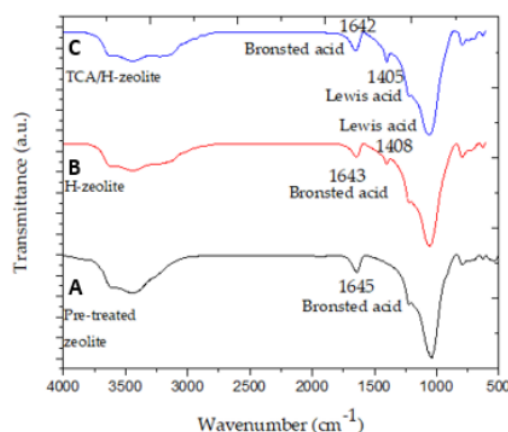
The total acidity of the TCA/H-zeolite catalyst was conducted through ammonia adsorption in combination with a gravimetric method. The amount of ammonia adsorbed at the catalyst surface would provide the data the number of acid active sites interacting with the adsorbed ammonia [27,28].

The total acidity of the TCA/H-zeolite catalyst in comparison with the pre-treated and H-zeolite is presented in Table 1. A significant increase in the total acidity of the TCA/H-zeolite catalyst was observed, 1.7 folds from that of H-zeolite. It was most likely due to the modification of the zeolite with TCA resulting in the chemical interaction of carbonyl oxygen or hydroxyl oxygen of TCA with the Brønsted acid sites of H-zeolite [29].

Table 1 The total acidity and the surface porosity of the zeolite catalysts.

Type of catalyst	Total acidity (mmol NH ₃ /g)	Surface area (m ² /g)	Total pore volume (cm ³ /g)	Average pore radius (Å)
Pre-treated zeolite	0.94	12.82	0.077	119.96
H-zeolite	1.20	22.26	0.065	588.35
TCA/H-zeolite	3.28	28.41	0.075	526.31

Furthermore, the interaction between ammonia Lewis's base and the Brønsted and Lewis sites of the catalyst was evaluated through the IR spectra of the TCA/H-zeolite catalyst in **Figure 3**. The interaction of ammonia with the Lewis and Brønsted active sites was designated by the vibrations at wavenumbers of 1,450 cm⁻¹ and 1,550 - 1,640 cm⁻¹, respectively [30].

**Figure 3** IR spectra of a) pre-treated zeolite, b) H-zeolite and c) TCA/H-zeolite after NH₃ adsorption.

The surface porosity of a catalyst is an important property of the catalyst in supporting the catalytic performance. It was due to the presence of active sites at the catalyst surface including the catalyst pores [31]. The surface porosity of the TCA/H-zeolite catalyst determined in this study included specific surface area, total pore volume and average pore radius of the catalyst as presented in **Table 1**.

The surface porosity data in **Table 1** showed that chemical and physical treatment towards the pre-treated zeolite caused a significant increase (73.63 %) in the surface area of the H-zeolite catalyst. It was might due to the impurity removal and the formation of new pores during the treatment [32]. A further increase (27.63 %) in the specific surface area was also observed in the TCA/H-zeolite catalyst, probably due to the surface modification using a strong acid TCA at the solid H-zeolite surface [33,34].

A significant increase of the average pore radius of the H-zeolite catalyst in comparison with the pre-treated zeolite catalyst (3.9 folds) was also observed. The acid treatment followed with calcination at high temperature of 500 °C probably could cause impurity removal resulting in an increase in the pore size of the zeolite [33]. Moreover, the growth of the pore structure might take place due to the chemical treatment during the preparation of the H-zeolite catalyst [35]. However, a slight decrease (~10 %) of the average pore radius was observed after the zeolite modification with TCA. The TCA introduction with a quite high concentration (ca. 35 %) at the H-zeolite surface followed with a low drying temperature (80 °C) might promote the pore occupation by the TCA molecules, resulting in the decrease of the average pore size of the zeolite [36].

Unlike the considerable changes in the specific surface area and average pore radius, the total pore volume of the zeolite catalysts was almost unchanged; only ~15 % of change was observed. The insignificant change in the total pore volume accompanied with the increase in the average pore radius might be probably attributed to the reduction of the pore depth at the zeolite surface. This would allow the easier interaction between the surface-active sites and the reactants during the esterification of the bio-oil.

1.1 Production and characterisation of the bio-oil from the fast pyrolysis of sengon wood sawdust

The bio-oil used as the feedstock during the esterification in this study was produced from the fast pyrolysis of Sengon wood sawdust with a particle size of 297 μm at 600 $^{\circ}\text{C}$ using a fixed-bed pyrolyser. The yield of the bio-oil was considerably high of 45.66 wt%, as presented in Table 2. Such high temperature would help the lignocellulose macromolecules to undergo good decomposition during the pyrolysis [37]. Lignocellulose composes of lignin, cellulose and hemicellulose with specific decomposition temperatures. Lignin would decompose at 300 - 550 $^{\circ}\text{C}$, while hemicellulose and cellulose would decompose at 250 - 350 and 325 - 400 $^{\circ}\text{C}$, respectively [38]. The rate of decomposition of lignocellulose macromolecules would increase with increasing the pyrolysis temperature, resulting in more condensable light fractions [39], thus high bio-oil yield. However, extremely high temperature would promote the production of the non-condensable fractions resulting in higher yield of gaseous pyrolysis product [40].

Table 2 The yield of pyrolysis products produced from the pyrolysis of Sengon wood sawdust with a particle size of 297 μm at 600 $^{\circ}\text{C}$ using a fixed-bed pyrolyser.

Type of product	Yield (wt.%)
Bio-oil	45.66
Biochar	29.97
Gaseous product*	24.37

*by difference

The physical and chemical properties of the Sengon wood bio-oil produced through fast pyrolysis technique were measured, including the density, viscosity, and total acid number as shown in Table 3. The density of the bio-oil was not directly related to the quality of the bio-oil. However, this property could provide an indication whether heavy or light molecules were predominant in the bio-oil [41]. The low density of the bio-oil produced in this study (1.07 g/mL) indicated that light molecules with relatively low molecular weight were predominant due to severe decomposition process at 600 $^{\circ}\text{C}$ during the pyrolysis resulting in more condensable light fractions.

Table 3 The characteristics of the bio-oil produced from the pyrolysis of Sengon wood sawdust with a particle size of 297 μm at 600 $^{\circ}\text{C}$ using a fixed-bed pyrolyser.

Property (unit)	Value (wt.%)
Density (g/mL)	1.07
Viscosity (cP)	2.40
TAN (mg KOH/g)	0.73

Another parameter evaluated in this study for the bio-oil quality is viscosity. This parameter is affected by the liquid temperature, the strength of intermolecular forces, and the molecular weight and the amount of the soluble components in the liquid bio-oil [42]. The pyrolysis temperature of 600 $^{\circ}\text{C}$ has resulted in the bio-oil with light components (short carbon chains, low molecular weight) in the considerable amount, resulting in the bio-oil with a low viscosity of 2.40 cP (see Table 3) [43].

The total acid number of the Sengon wood bio-oil was determined by using an aliquot method, as presented in Table 3. This parameter provided an estimation of the content of organic acids in the bio-oil [44]. The high content of organic acids in bio-oil or liquid fuels would lead to corrosion to engines and/or

the equipment used in the further processes such as biorefinery [8]. The high total acid number (0.73 mg/g) of the Sengon wood bio-oil used as the feedstock in the esterification process suggested the high organic acid content in the bio-oil. It was likely due to the presence of organic acids such as carboxylic acids as a result of the decomposition of the lignocellulose macromolecules at higher pyrolysis temperature [45]. The acid removal from the bio-oil is extremely important to minimise the corrosiveness of the bio-oil prior to its use as a fuel or its further processes in the biorefinery through an appropriate upgrading technique. A bio-oil upgrading through an esterification technique using TCA/H-zeolite was investigated with different weight ratios of bio-oil-to-methanol over various reaction times.

Bio-oil upgrading through TCA/H-zeolite-catalysed esterification over different weight ratios of bio-oil-to-methanol

The esterification of the Sengon wood bio-oil in the presence of the TCA/H-zeolite catalyst was carried out with various weight ratios of bio-oil-to-methanol of 2:1, 1:1, 1:2 and 1:3 at 70 °C, a catalyst loading of 10 wt%, a 60-min reaction time, and a stirring rate of 500 rpm. The liquid and the possible formed coke after each esterification experiment were recovered to close the mass balance, as presented in Table 4. The mass balance closure was higher than 90 wt% indicating a proper experimental execution [46]. The coke yield in all experiments was very low of < 1 wt%. This indicated that the possible repolymerisation between the reactive components in the bio-oil leading to the formation of coke could be prevented during the bio-oil esterification [47] in the presence of the TCA/H-zeolite catalyst.

Table 4 The mass balance closure during the esterification of the sengon wood bio-oil in the presence of TCA/H-zeolite catalyst with various weight ratios of bio-oil-to-methanol.

Weight ratio of BO-to-methanol	Recovered liquid (wt%)	Coke yield (wt%)	Total recovery (%)
2:1	94.11	0.0407	94.15
1:1	91.90	0.0404	91.94
1:2	91.88	0.0394	91.92
1:3	97.79	0.0334	97.82

The density, viscosity and total acid number of the liquid obtained after the TCA/H-zeolite-catalysed esterification with various weight ratios of bio-oil-to-methanol at 70 °C were measured as presented in Table 5. A catalyst loading of 10 wt%, a 60-min reaction time, and a stirring rate of 500 rpm were employed during each experiment. The density of the esterified oil insignificantly changed with relatively abundant addition of methanol compared to the original mixture of the bio-oil and methanol before reaction in the case of the experiments with a weight ratio of bio-oil-to-methanol of 1:2 and 1:3. The relatively unchanged density indicated the relatively similar molecular weight of components in the bio-oil after esterification. The esterification would allow the change in the bio-oil microstructure through the formation of esters or acetals [48]. The similar trend was observed for the viscosity of the esterified oil; the more the methanol added during the esterification, the lower the change in the viscosity of the bio-oil. The presence of methanol could enhance the bio-oil stability [49] and further decrease the rate of aging during storage [50].

Table 5 The density, viscosity and total acid number of the bio-oil after esterification in the presence of TCA/H-zeolite catalyst with various weight ratios of bio-oil-to-methanol.

Bio-oil property	Weight ratio of bio-oil-to-methanol							
	2:1		1:1		1:2		1:3	
	Initial	Final	Initial	Final	Initial	Final	Initial	Final
Density (g/mL)	1.0227	1.0252	0.9861	0.9866	0.9415	0.9417	0.9153	0.9186
Viscosity (cP)	2.1094	2.2316	1.9417	2.0283	1.7896	1.8521	1.5643	1.6034
TAN (mg/g)	0.6921	0.3498	0.5852	0.2939	0.5316	0.2031	0.4132	0.1813

Unlike the insignificant changes in the bio-oil density and viscosity, a considerable change in the total acid number of the esterified oil was observed after the esterification in the presence of the TCA/H-zeolite catalyst, as presented in Table 5. The decrease in the total acid number of the bio-oil after esterification was 49.46, 49.78, 61.79 and 56.12 % for the TCA/H-zeolite-catalysed esterification with a bio-oil-to-methanol weight ratio of 2:1, 1:1, 1:2 and 1:3 respectively. The addition of extra methanol in the esterification with a 1:2 weight ratio could promote the decrease in the total acid number of the bio-oil by ca 25 % in comparison with that with a 2:1 and 1:1 weight ratio. The decrease in the total acid number of the bio-oil after esterification could be an indication of the formation of esters as a result of the reaction between carboxylic acids in the bio-oil feedstock and methanol in the presence of the TCA/H-zeolite catalyst [51]. In addition, aldehydes in the bio-oil feedstock could also react with methanol in the presence of acid catalysts, such as TCA/H-zeolite catalyst, to form acetals [52]. The extra addition of methanol in the esterification system (in the case of that with a 1:2 and 1:3 weight ratio) could promote the equilibrium shift to the products, resulting in the increase in the production of products, i.e., esters or acetals [53]. A further increase in the methanol addition in the esterification with a 1:3 weight ratio did not cause a higher decrease in the total acid number of the bio-oil after esterification in the presence of the TCA/H-zeolite catalyst. It might indicate that the equilibrium was not disturbed by the extra addition of methanol in the 1:3 esterification experiment. The weight ratio of bio-oil-to-methanol of 1:2 was then chosen as the condition in the further experiments with various reaction times.

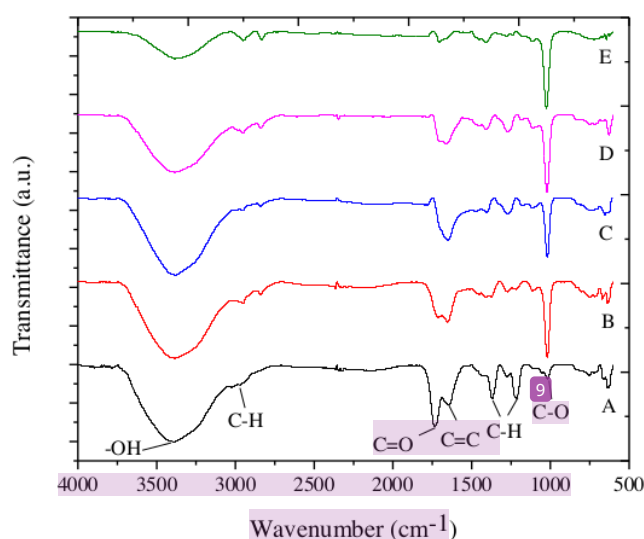


Figure 4 The IR spectra of (A) the fresh bio-oil and the bio-oils after esterification with a weight ratio of bio-oil-to-methanol of (B) 2:1, (C) 1:1, (D) 1:2 and (E) 1:3 in the presence of the TCA/H-zeolite catalyst.

Further observation on the possible formation of esterification products, e.g., esters, an FTIR measurement was conducted towards the fresh bio-oil (the bio-oil before the esterification) and the bio-oils after the esterification with different weight ratios of bio-oil-to-methanol in the presence of the TCA/H-zeolite catalyst. The IR spectra of the fresh and esterified bio-oils are depicted in Figure 4. A considerable increase in the peak intensity of the hydroxyl and C-H alkane groups at wavenumbers of $3,350\text{ cm}^{-1}$ and $2,950 - 2,800\text{ cm}^{-1}$, respectively, in the esterified bio-oils (Figures 4(B) - 4(E)) was observed, possibly due to the formation of esters [54]. In addition, a significant increase in the peak intensity of C-O groups at a wavenumber of $1,000\text{ cm}^{-1}$ was observed as an indication of the presence of methanol in the reaction system, as well as the formation of ester [53]. Meanwhile, the decrease in the peak intensity at a wavenumber of $1,750\text{ cm}^{-1}$ designated for the carbonyl groups from carboxylic acids, aldehydes and ketones [52], possibly due to its conversion to acetals [55,56].

7 Bio-oil upgrading through TCA/H-zeolite-catalysed esterification over different reaction times

The esterification of the Sengon wood bio-oil in the presence of the TCA/H-zeolite catalyst over different reaction times at 70 °C with a catalyst loading of 10 wt%, a weight ratio of bio-oil-to-methanol of 1:2, stirring rate of 500 rpm was carried out with a total recovery of > 90 %, as listed in Table 6, indicating a proper experimental execution. The recovered liquid contained the esterification products and possible remaining reactants. Table 6 shows that the coke yield was very low (< 1 wt%), indicating that the coke formation during the bio-oil esterification in the presence of the TCA/H-zeolite could be avoided [53].

Over prolonged reaction times, the density of the bio-oil after esterification underwent a negligible change, only by < 1 %, possibly due to the enhanced stability of the bio-oil during the esterification as is shown in Table 7. The susceptibility of the reactive components of the bio-oil towards re-polymerisation has lowered resulting in the bio-oil with similar compositions of molecular weight [57].

Table 6 The mass balance closure during the esterification of the Sengon wood bio-oil in the presence of TCA/H-zeolite catalyst for 15 - 60 min reaction times.

Reaction time (min)	Recovered liquid (wt%)	Coke yield (wt%)	Total (%)
15	92.95	0.0354	92.98
30	95.34	0.0370	95.38
45	92.92	0.0375	92.96
60	91.88	0.0394	91.92

Table 7 The density, viscosity and total acid number of the bio-oil after esterification in the presence of TCA/H-zeolite catalyst for 15 - 60 min reaction times.

Bio-oil property	Esterification time (min)							
	15		30		45		60	
	Initial	Final	Initial	Final	Initial	Final	Initial	Final
Density (g/mL)	0.9394	0.9399	0.9393	0.9401	0.9393	0.9406	0.9415	0.9417
Viscosity (cP)	1.7748	1.7908	1.7789	1.8040	1.7704	1.8308	1.7896	1.8521
TAN (mg/g)	0.5074	0.2646	0.5161	0.2588	0.5196	0.2241	0.5316	0.2032

The similar trend was observed for the viscosity of the bio-oil after esterification in the presence of the TCA/H-zeolite over various reaction times at 70 °C with a catalyst loading of 10 wt%, a weight ratio of bio-oil-to-methanol of 1:2, stirring rate of 500 rpm. Insignificant changes in the bio-oil viscosity by 3 - 5 % were observed, indicating the prevention of the formation of heavy molecules during the catalysed esterification, possibly by the formation of esters and acetals [48].

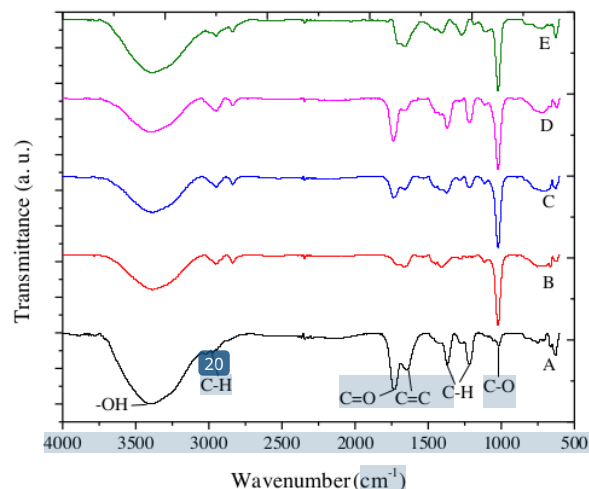


Figure 5 The IR spectra of the bio-oils after a (A) 0-min, (B) 15-min, (C) 30-min, (D) 45-min and (E) 60-min esterification in the presence of the TCA/H-zeolite catalyst.

17 Alike the change in the total acid number of the bio-oil after esterification with various weight ratios of bio-oil-to-methanol, the total acid number of the bio-oil after the esterification over various reaction times decreased considerably. Over a 15-min reaction time, the total acid number of the bio-oil after the catalysed esterification decreased by 47.85 %. A prolonged esterification of 30 min only caused a further decrease in the total acid number of the bio-oil 4 % (with a 49.85 % decrease). A further prolonged reaction times of 45 and 60 min caused a bit higher decrease in the total acid number of bio-oil by 13 and 8 %, respectively (with 56.78 and 61.78 % decrease, respectively). These data suggested that carboxylic acids in the bio-oil feedstock were converted to esters in a quite fast rate at the beginning of the esterification of the bio-oil in the presence of TCA/H-zeolite catalyst [51]. The rate of esterification became slower by longer reaction times (30 - 60 min). Probably, the components of the bio-oil feedstock competed to attach to the active sites of the catalysts over time resulting in the high surface coverage [58]. However, not all of these reactants adsorbed at the catalyst surface could be accommodate to react with methanol as the co-adsorbed alcohol-acids intermediates at the catalyst surface were required to allow the reactions to take place [10].

A measurement using an FTIR spectrophotometer was conducted towards the fresh bio-oil and the bio-oils obtained after the TCA/H-zeolite-catalysed esterification over different reaction times. The IR spectra of the bio-oils before and after esterification over different reaction times are presented in Figure 5. A similar observation of the IR spectra with those in Figure 4 was obtained. An increase in the peak intensity of the hydroxyl and C-H groups at wavenumbers of 3,350 and 2,950 - 2,800 cm^{-1} , respectively, was observed in Figure 5, indicating the formation of water as a side-product of esterification between methanol and carboxylic acids [55,56]. The formation of esters was also indicated by the increase in the C-O groups at a wavenumber of 1,000 cm^{-1} [53]. Moreover, the carbonyl-containing compounds as designated the peaks at a wavenumber 1,750 cm^{-1} [53] in the bio-oil were possibly converted to acetals [55], as indicated by the decrease in the corresponding peak intensity.

Comparing the activity of zeolite catalysts during the esterification of sengon wood bio-oil

The activity of the TCA/H-zeolite catalyst during the esterification of the Sengon wood sawdust was confirmed by comparing to that of the pre-treated zeolite and H-zeolite catalysts. The study was performed using the following condition: a temperature of 70 °C, a weight ratio of bio-oil-to-methanol of 1:2 and a reaction time of 60 min. A blank experiment in the absence of any catalyst was also carried out to support the justification on the performance of the TCA/H-zeolite catalyst. The liquid after esterification as well as the possible formed coke was recovered and weighed to close the mass balance as presented in Table 8.

Table 8 The mass balance closure during the esterification of the Sengon wood bio-oil in the presence of various catalysts.

Type of catalyst	Recovered liquid (wt%)	Coke Yield (wt%)	Total (%)
NA	94.42	0.016	94.44
Pre-treated zeolite	93.18	0.043	93.23
H-zeolite	94.90	0.041	94.94
TCA/H-zeolite	91.88	0.039	91.92

The data in **Table 8** suggested that negligible coke formation (< 1 %) was observed. The presence of methanol during the heating up bio-oil was significant in preventing the re-polymerisation of reactive components in the bio-oil feedstock. The good mass balance closure in **Table 8** indicated that the experiments were carried out properly. The properties of the bio-oil after the esterification of bio-oil in the presence of various zeolite catalysts at 70 °C with a catalyst loading of 10 wt%, a weight ratio of bio-oil-to-methanol of 1:2, stirring rate of 500 rpm for a 60-min reaction time were investigated as listed in **Table 9**.

Table 9 The density, viscosity and total acid number of the bio-oil after esterification in the presence of the zeolite catalysts.

Bio-oil property	Reaction time (min)	Type of catalyst			
		NA	Pre-treated zeolite	H-zeolite	TCA/H-zeolite
Density(g/mL)	0	0.9176	0.9101	0.9140	0.9415
	60	0.9179	0.9347	0.9392	0.9417
Viscosity (cP)	0	1.7336	1.7257	1.7373	1.7896
	60	1.8367	2.3055	2.1174	1.8521
TAN (mg/g)	0	0.7006	0.6515	0.5731	0.5316
	60	0.5947	0.4240	0.2843	0.2032

The density of the bio-oil after the esterification in **Table 9** showed an insignificant change even in the absence of a catalyst. It suggested that the addition of methanol have a significant effect in stabilising the reactive component of the bio-oil [53]. In contrast, the viscosity of the bio-oil after esterification in the presence and absence of a catalyst has increased in a different level ranging from 3.94 - 39.97 %. The lowest increase in the viscosity of the bio-oil after esterification was observed for that in the presence of the TCA/H-zeolite catalyst (3.94 %), while the highest increase was observed for that in the presence of the pre-treated zeolite catalyst (39.97 %). The blank experiment in the absence of a catalyst did not show a significant increase in the viscosity of the bio-oil after esterification possibly due to the limited interaction of the reactive components in the bio-oil feedstock with methanol [59]. On the other hand, the presence of the zeolite catalysts might promote the interaction between reactive components themselves or with methanol [23]. The pre-treated zeolite might facilitate the interaction between reactive components to polymerise and form bigger molecules with higher molecular weight. As a result, the viscosity of the bio-oil increased significantly after esterification in the presence of the pre-treated zeolite catalyst.

The bio-oil esterification in the presence of zeolite catalysts (pre-treated, H-zeolite and TCA/H-zeolite catalysts) showed a significant decrease in the total acid number of the bio-oil after esterification by 34.92, 50.39 and 61.78 %, respectively. It was clear that the modification of Indonesian zeolite using TCA could enhance its activity in catalysing the esterification of the Sengon wood bio-oil. It was possibly due to the increase in the acid active sites at the catalyst surface as the result of the TCA modification over the zeolite catalyst [60].

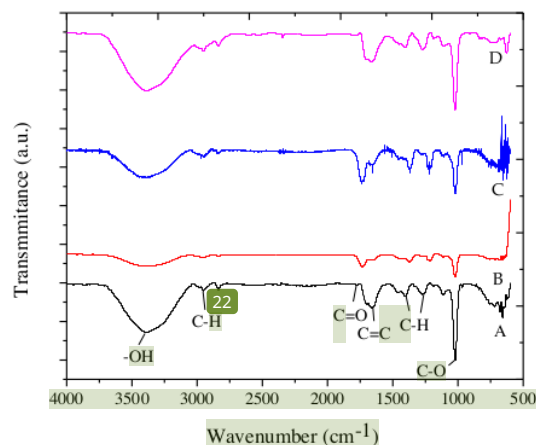


Figure 6 The IR spectra of the esterified bio-oils in the presence of (A) no catalyst, (B) pre-treated zeolite, (C) H-zeolite and (E) the TCA/H-zeolite catalysts.

The change in the functionalities of the bio-oils before and after the esterification of the bio-oils in the absence and presence of a catalyst was investigated using an FTIR spectrophotometer, as presented in Figure 6. The high peak intensity of the C-O groups in the esterified bio-oils in Figure 6 indicated the formation of esters [53]. The presence of the TCA/H-zeolite did promote the formation of esters (and possibly other esterification products, e.g., acetals [56]) in comparison with that of other zeolite catalysts.

Conclusions

This study investigated the activity of TCA/H-zeolite catalyst during the bio-oil esterification in the presence of methanol of various weight ratios of bio-oil-to-methanol and reaction times. The presence of TCA/H-zeolite catalyst during the esterification of the bio-oil could suppress the formation of coke. In the presence of TCA/H-zeolite, the weight ratios of bio-oil-to-methanol significantly affected the decrease in the total acid number of the bio-oil after the esterification. Moreover, the esterification of *Sc* on wood bio-oil in the presence of the TCA/H-zeolite catalyst took place in a fast rate, indicated by the decrease in the total acid number of the bio-oil by 47.85 % over a 15-min esterification. Compared to the uncatalysed esterification, the presence of the TCA/H-zeolite catalyst could further enhance the decrease in the total acid number up to 65.83 %.

The esterification at higher temperatures and using a pressurised reactor would improve the quality of the esterified bio-oil. Furthermore, the combination between hydrocracking and esterification could simultaneously undergo in the presence of hydrogen and hydroprocessing catalysts.

Acknowledgements

The authors would like to thank the Research and Community Service Institute, Universitas Negeri Semarang for the financial support through “Penelitian Dasar” scheme 2021 with a contract number of 262.26.4/UN37/PPK.3.1/2021. This study has also received a support from the Directorate General of Higher Education of the Republic of Indonesia through “Penelitian Dasar Unggulan Perguruan Tinggi (PDUPT)” 2021 with a contract number of 132/SP2H/LT/DRPM/2021; 132/E4.1/AK.04.PT/2021 and derivate contract number of 23.14.7/UN37/PPK.6.8/2021. The authors are also very grateful for the kind help from Ms. Y.M. Rosanti for the experimental facilities.

References

- [1] CL Williams, A Dahiya and P Porter. *Introduction to bioenergy*. In: A Dahiya (Ed.). Bioenergy biomass to biofuels. Academic Press, Massachusetts, 2015, p. 5-36.
- [2] N Canabarro, JF Soares, CG Anchieta, CS Kelling and MA Mazutti. Thermochemical processes for biofuels production from biomass. *Sustain. Chem. Process.* 2013; **1**, 22.
- [3] NS Hartati, E Sudarmonowati, W Fatriasari, E Hermiati, W Dwianto, R Kaida, K Baba and T Hayashi. Wood characteristic of superior Sengon collection and prospect of wood properties improvement through genetic engineering. *Wood Res. J.* 2010; **1**, 103-7.
- [4] RE Guedes, AS Luna and AR Torres. Operating parameters for bio-oil production in biomass pyrolysis: A review. *J. Anal. Appl. Pyrol.* 2018; **129**, 134-49.
- [5] A Pattiya. *Fast pyrolysis*. In: L Rosendahl (Ed.). Direct thermochemical liquefaction for energy applications. Woodhead Publishing, Sawston, 2018, p. 3-28.
- [6] G Lyu, S Wu and H Zhang. Estimation and comparison of bio-oil components from different pyrolysis conditions. *Front. Energy Res.* 2015; **3**, 1-11.
- [7] GH Wienhage, ES Ramos, LM Chiarello, V Botton and VR Wiggers. Acidity reduction of bio-oil by methylic esterification reactions. *Oil Gas J.* 2021; **2**, 21-27.
- [8] NL Panwar and AS Paul. An overview of recent development in bio-oil upgrading and separation techniques. *Environ. Eng. Res.* 2021; **26**, 200382.
- [9] X Hu. *Stabilization of bio-oil via esterification in chemical catalysts for biomass upgrading*. In: M Crocker and E Santillan-Jimenez (Eds.). Chemical catalysts for biomass upgrading. Wiley Online Library, New Jersey, 2019, p. 97-144.
- [10] L Ciddor, JA Bennett, JA Hunns, K Wilson and AF Lee. Catalytic upgrading of bio-oils by esterification. *J. Chem. Tech. Biotechnol.* 2015; **90**, 780-95.
- [11] Y Liu, Z Li, JJ Leahy and W Kwapinski. Catalytically upgrading bio-oil via esterification. *Energy Fuel.* 2015; **29**, 3691-8.
- [12] JJ Wang, J Chang and J Fan. Catalytic esterification of bio-oil by ion exchange resins. *J. Fuel Chem. Tech.* 2010; **38**, 560-4.
- [13] W Thitsartarn and S Kawi. Transesterification of oil by sulfated Zr-supported mesoporous silica. *Ind. Eng. Chem. Res.* 2011; **50**, 7857-65.
- [14] M Kim, C Dimaggio, SO Salley and N Simon. A new generation of zirconia supported metal oxide catalysts for converting low grade renewable feedstocks to biodiesel. *Bioresource Tech.* 2012; **118**, 37-42.
- [15] P Weerachanchai, C Tangsathitkulchai and M Tangsathitkulchai. Effect of reaction conditions on the catalytic esterification of bio-oil. *Kor. J. Chem. Eng.* 2012; **29**, 182-9.
- [16] X Hu, R Gunawan, D Mourant, C Lievens, X Li, S Zhang, W Chaiwat and CZ Li. Acid-catalysed reactions between methanol and the bio-oil from the fast pyrolysis of mallee bark. *Fuel* 2012; **97**, 512-22.
- [17] L Wu, X Hu, S Wang, D Mourant, Y Song, T Li and CZ Li. Formation of coke during the esterification of pyrolysis bio-oil. *RSC Adv.* 2016; **6**, 86485-93.
- [18] B Sutrisno and A Hidayat. Upgrading of bio-oil from the pyrolysis of biomass over the rice husk ash catalysts. *IOP Conf. Mater. Sci. Eng.* 2016; **162**, 012014.
- [19] P Prasertpong and N Tippayawong. Upgrading of biomass pyrolysis oil model compound via esterification: kinetic study using heteropoly acid. *Energy Procedia* 2019; **160**, 253-9.
- [20] M Milina, S Mitchell and J Pérez-Ramírez. Prospectives for bio-oil upgrading via esterification over zeolite catalysts. *Catal. Today* 2014; **235**, 176-83.
- [21] KY Nandiwale, SK Sonar, PS Niphadkar, PN Joshi, SS Deshpande, VS Patil and VV Bokade. Catalytic upgrading of renewable levulinic acid to ethyl levulinate biodiesel using dodecatungstophosphoric acid supported on desilicated H-ZSM-5 as catalyst. *Appl. Catal. Gen.* 2013; **460-461**, 90-8.
- [22] N Fattahi, K Triantafyllidis, R Luque and A Ramazani. Zeolite-based catalysts: A valuable approach toward ester bond formation. *Catalysts* 2019; **9**, 758.
- [23] A Osatiashiani, B Puértolas, CCS Oliveira, JC Manayil, B Barbero, M Isaacs, C Michailof, E Heracleous, J Pérez-Ramírez, AF Lee and K Wilson. On the influence of Si: Al ratio and hierarchical porosity of FAU zeolites in solid acid catalysed esterification pre-treatment of bio-oil. *Biomass Convers. Biorefinery* 2017; **7**, 331-42.

- [24] S Kadarwati, E Apriliani, RN Annisa, J Jumaeri, E Cahyono and S Wahyuni. Esterification of bio-oil produced from sengon (*Paraserianthes falcataria*) wood using Indonesian natural zeolites. *Int. J. Renew. Energ. Dev.* 2021; **10**, 747-54.
- [25] JM Müller, GC Mesquita, SM Franco, LD Borges, JLD Macedo, JA Dias and SCL Dias. Solid-state dealumination of zeolites for use as catalysts in alcohol dehydration. *Microporous Mesoporous Mater.* 2014; **204**, 50-7.
- [26] MC Ávila, NA Comelli, E Rodríguez-castellón, A Jiménez-López, RC Flores, EN Ponzi and MI Ponzi. Study of solid acid catalysis for the hydration of α -pinene. *J. Mol. Catal. Chem.* 2010; **322**, 106-12.
- [27] IV Mishin, TR Brueva and GI Kapustin. Heats of adsorption of ammonia and correlation of activity and acidity in heterogeneous catalysis. *Adsorption* 2005; **11**, 415-24.
- [28] F Giraud, C Geantet, N Guilhaume, S Loridant, S Gros, L Porcheron, M Kanniche and D Bianchi. Individual amounts of lewis and Brønsted acid sites on metal oxides from NH₃ adsorption equilibrium: Case of TiO₂ based solids. *Catal. Today* 2021; **373**, 69-79.
- [29] X Li, Y Zhao, S Wang, Y Zhu and G Yang. DFT-D₂ study of the adsorption of bio-oil model compounds in HZSM-5: C1–C4 carboxylic acids. *Catal. Lett.* 2016; **146**, 2015-24.
- [30] P Concepción. *Application of infrared spectroscopy in catalysis: Impacts on catalysts' selectivity.* In: M El-Azazy (Ed.). *Infrared spectroscopy.* IntechOpen, London, 2018.
- [31] Y Pan, X Shen, L Yao, A Bentalib and Z Peng. Active sites in heterogeneous catalytic reaction on metal and metal oxide: theory and practice. *Catal* 2018; **8**, 478.
- [32] H Karami, M Kazemeini, S Soltanali and M Rashidzadeh. The effect of acid treatment and calcination on the modification of zeolite X in diesel fuel hydrodesulphurization. *Can. J. Chem. Eng.* 2022; **100**, 3357-66.
- [33] R Zakaria, NA Jamalluddin and MZA Bakar. Effect of impregnation ratio and activation temperature on the yield and adsorption performance of mangrove based activated carbon for methylene blue removal. *Res. Mater.* 2021; **10**, 100183.
- [34] S Bhati, JS Mahur, S Dixit and ON Chobey. Study on effect of chemical impregnation on the surface and porous characteristics of activated carbon fabric prepared from viscose rayon. *Carbon Lett.* 2014; **15**, 45-9.
- [35] A Mara, K Wijaya, W Trisunaryati and M Mudasar. Effect of sulfuric acid treatment and calcination on natural zeolites of Indonesia. *Asian J. Chem.* 2016; **28**, 11-4.
- [36] M Börnhorst, P Walzel, A Rahimi, A Kharaghani, E Tsotsas, N Nestle, A Besser, FK Jäger and T Metzger. Influence of pore structure and impregnation-drying conditions on the solid distribution in porous support materials. *Drying Tech.* 2016; **34**, 1964-78.
- [37] HLO Jr, FG Ornaghi, RM Neves, F Monticeli and O Bianchi. Mechanisms involved in thermal degradation of lignocellulosic fibers: a survey based on chemical composition. *Cellulose* 2020; **27**, 4949-61.
- [38] T Kan, V Strezov and TJ Evans. Lignocellulosic biomass pyrolysis: A review of product properties and effects of pyrolysis parameters. *Renew. Sustain. Energ. Rev.* 2016; **57**, 1126-40.
- [39] YH Chan, S Yusup, AT Quitain, Y Uemura and M Sasaki. Bio-oil production from oil palm biomass via subcritical and supercritical hydrothermal liquefaction. *J. Supercritical Fluid.* 2014; **95**, 407-12.
- [40] D Shen, R Xiao, H Zhang and S Gu. *The overview of thermal decomposition of cellulose in lignocellulosic biomass.* In: TGMVD Ven and J Kadla (Eds.). *Cellulose-biomass conversion.* IntechOpen, London, 2013.
- [41] JJ Thomas, HM Jennings and AJ Allen. Relationships between composition and density of tobermorite, jennite, and nanoscale CaO–SiO₂–H₂O. *J. Phys. Chem. C* 2010; **114**, 7594-601.
- [42] M Kawahigashi and N Fujitake. Relationship between viscosity and molecular weight in an andosol humic acid. *Soil Sci. Plant Nutr.* 2001; **47**, 399-404.
- [43] A Nofiyanto, G Soebiyakto and P Suwandono. Studi proses pirolisis berbahan jerami padi terhadap hasil produksi char dan tar sebagai bahan bakar alternatif. *Proton* 2019; **11**, 21-8.
- [44] LKE Park, J Liu, S Yiacoumi, AP Borole and C Tsouris. Contribution of acidic components to the total acid number (TAN) of bio-oil. *Fuel* 2017; **200**, 171-81.
- [45] SW Banks and AV Bridgwater. *Catalytic fast pyrolysis for improved liquid quality.* In: R Luque, CSK Lin, K Wilson and J Clark (Eds.). *Handbook of biofuels production (Second Edition).* Woodhead Publishing, Sawston, 2016, p. 391-429.
- [46] C Ovalles, E Rogel, H Morazan and ME Moir. *The importance of mass balances: Case studies of evaluation of asphaltene dispersants and antifoulants.* In: C Ovalles and ME Moir (Eds.). The

- Boduszynski continuum: Contributions to the understanding of the molecular composition of petroleum. American Chemical Society, Washington, 2018, p. 25-49.
- [47] X Hu, Z Zhang, M Gholizadeh, S Zhang, CH Lam, Z Xiong and Y Wang. Coke formation during thermal treatment of bio-oil. *Energ. Fuels* 2020; **34**, 7862-914.
- [48] D Chen, J Zhou, Q Zhang and X Zhu. Evaluation methods and research progresses in bio-oil storage stability. *Renew. Sustain. Energ. Rev.* 2014; **40**, 69-79.
- [49] Y Mei, M Chai, C Shen, B Liu and R Liu. Effect of methanol addition on properties and aging reaction mechanism of bio-oil during storage. *Fuel* 2019; **244**, 499-507.
- [50] LW Simões, NT Miranda, RM Filho and MR Wolf. Upgrading technique of sugarcane bagasse bio-oil heavy fraction for stability improvement. *Chem. Eng. Trans.* 2020; **80**, 49-54.
- [51] J Xu, J Jiang, W Dai, T Zhang and Y Xu. Bio-oil upgrading by means of ozone oxidation and esterification to remove water and to improve fuel characteristics. *Energ. Fuel.* 2011; **25**, 1798-801.
- [52] S Zhang, X Yang, H Zhang, C Chu, K Zheng, M Ju and L Liu. Liquefaction of biomass and upgrading of bio-oil: A review. *Molecules* 2019; **24**, 2250.
- [53] X Zhang, L Chen, W Kong, T Wang, Q Zhang, J Long, Y Xu and L Ma. Upgrading of bio-oil to boiler fuel by catalytic hydrotreatment and esterification in an efficient process. *Energy* 2015; **8**, 83-90.
- [54] SK Tanneru, DR Parapati and PH Steele. Pretreatment of bio-oil followed by upgrading via esterification to boiler fuel. *Energy* 2014; **73**, 214-20.
- [55] L Moens, SK Black, MD Myers and S Czernik. Study of the neutralization and stabilization of a mixed hardwood bio-oil. *Energ. Fuel.* 2009; **23**, 2695-9.
- [56] S Omar, S Alsamaq, Y Yang and J Wang. Production of renewable fuels by blending bio-oil with alcohols and upgrading under supercritical conditions. *Chem. Sci. Eng.* 2019; **13**, 702-17.
- [57] L Zhang, R Liu, R Yin, Y Mei and J Cai. Optimization of a mixed additive and its effect on physicochemical properties of bio-oil. *Chem. Eng. Tech.* 2014; **37**, 1181-90.
- [58] R Asadpour, NB Sapari, MH Isa, S Kakooei and KU Orji. Acetylation of corn silk and its application for oil sorption. *Fibers Polymer.* 2015; **16**, 1830-5.
- [59] F Wenting, L Ronghou, Z Weiqi, M Yuanfei and Y Renzhan. Influence of methanol additive on bio-oil stability. *Int. J. Agr. Biol.* 2014; **7**, 83-92.
- [60] X Lian, Y Xue, Z Zhao, G Xu, S Han and H Yu. Progress on upgrading methods of bio-oil: A review. *Int. J. Energ. Res.* 2017; **41**, 1798-816.

ORIGINALITY REPORT

16%

SIMILARITY INDEX

12%

INTERNET SOURCES

13%

PUBLICATIONS

3%

STUDENT PAPERS

PRIMARY SOURCES

1	espace.curtin.edu.au Internet Source	2%
2	Heuntae Jo, Hermawan Prajitno, Hassan Zeb, Jaehoon Kim. "Upgrading low-boiling-fraction fast pyrolysis bio-oil using supercritical alcohol: Understanding alcohol participation, chemical composition, and energy efficiency", Energy Conversion and Management, 2017 Publication	2%
3	Submitted to Universitas Muhammadiyah Semarang Student Paper	1%
4	Yejin Lee, Hoda Shafaghat, Jae-kon Kim, Jong-Ki Jeon, Sang-Chul Jung, In-Gu Lee, Young-Kwon Park. "Upgrading of pyrolysis bio-oil using WO ₃ /ZrO ₂ and Amberlyst catalysts: Evaluation of acid number and viscosity", Korean Journal of Chemical Engineering, 2017 Publication	1%
5	Junmeng Cai, Md. Maksudur Rahman, Shukai Zhang, Manobendro Sarker, Xingguang	1%

Zhang, Yuqing Zhang, Xi Yu, Elham H. Fini.
"Review on Aging of Bio-Oil from Biomass
Pyrolysis and Strategy to Slowing Aging",
Energy & Fuels, 2021

Publication

6	coek.info Internet Source	1 %
7	Staš, Martin, David Kubička, Josef Chudoba, and Milan Pospíšil. "Overview of Analytical Methods Used for Chemical Characterization of Pyrolysis Bio-oil", Energy & Fuels, 2014. Publication	1 %
8	"Nano- and Biocatalysts for Biodiesel Production", Wiley, 2021 Publication	1 %
9	etheses.whiterose.ac.uk Internet Source	1 %
10	grad.wu.ac.th Internet Source	1 %
11	ris.utwente.nl Internet Source	<1 %
12	Mark Daniel G. de Luna, Louie Angelo D. Cruz, Wei-Hsin Chen, Bo-Jhih Lin, Tzu-Hsien Hsieh. "Improving the stability of diesel emulsions with high pyrolysis bio-oil content by alcohol co-surfactants and high shear mixing strategies", Energy, 2017	<1 %

13

Wan Pyo Hong, Jae Yeon Park, Kyoungseon Min, Myung Joo Ko, Kyungmoon Park, Young Je Yoo. "Kinetics of glycerol effect on biodiesel production for optimal feeding of methanol", Korean Journal of Chemical Engineering, 2011

Publication

<1 %

14

www.science.gov

Internet Source

<1 %

15

Hongli Tian, Yuewen Shao, Chuanfei Liang, Qing Xu, Lijun Zhang, Shu Zhang, Shuhua Liu, Xun Hu. "Sulfated attapulgite for catalyzing the conversion of furfuryl alcohol to ethyl levulinate: Impacts of sulfonation on structural transformation and evolution of acidic sites on the catalyst", Renewable Energy, 2020

Publication

<1 %

16

Liping Wu, Xun Hu, Shuai Wang, M.D. Mahmudul Hasan, Shengjuan Jiang, Tingting Li, Chun-Zhu Li. "Acid-treatment of bio-oil in methanol: The distinct catalytic behaviours of a mineral acid catalyst and a solid acid catalyst", Fuel, 2018

Publication

<1 %

17

Narayan Lal Panwar, Arjun Sanjay Paul. "An overview of recent development in bio-oil

<1 %

upgrading and separation techniques", Environmental Engineering Research, 2020

Publication

18 lp2m.unnes.ac.id <1 %
Internet Source

19 epdf.tips <1 %
Internet Source

20 vital.seals.ac.za:8080 <1 %
Internet Source

21 F. A. Agblevor, H. Wang, S. Beis, K. Christian,
A. Slade, O. Hietsoi, D. M. Santosa. "
Reformulated Red Mud: a Robust Catalyst for
Catalytic Pyrolysis of Biomass ", Energy &
Fuels, 2020
Publication

22 www.electrochemsci.org <1 %
Internet Source

23 R. Kumar, V. Strezov. "Thermochemical
production of bio-oil: A review of downstream
processing technologies for bio-oil upgrading,
production of hydrogen and high value-added
products", Renewable and Sustainable Energy
Reviews, 2021
Publication

24 docplayer.biz.tr <1 %
Internet Source

25

pubs.rsc.org

Internet Source

<1 %

26

worldwidescience.org

Internet Source

<1 %

Exclude quotes On

Exclude matches < 20 words

Exclude bibliography On